10th INTERNATIONAL SCIENTIFIC CONFERENCE
ON DEFENSIVE TECHNOLOGIES
OTEH 2022
Belgrade, Serbia, 13 – 14 October 2022

BIRDS AND DRONES SPECTROGRAMS AND HOW TO DIFFER THEM

JOVAN RADIVOJEVIĆ
IRITEL a.d., Belgrade, jovan.radivojevic@iritel.com

DEJAN STANOJEVIĆ
IRITEL a.d., Belgrade, dejan.stanojevic@iritel.com

ALEKSANDAR LEBL
IRITEL a.d., Belgrade, lebl@iritel.com

Abstract: *FMCW radar spectrograms are powerful technique for malicious drones detection and identification. But, there is a high risk that drones are replaced by birds and vice versa. The original analytical procedure for birds spectrogram calculation is presented in this paper. The developed expressions are similar to the known corresponding expressions for drones. These expressions are suitable to hovering drones and birds whose only movement is related to flapping wings. It is analyzed how physical characteristics and motion performances of both targets influence their spectrogram appearance. The obtained spectrograms for drones and birds are mutually compared and some recommendations for their distinguishing are emphasized.*

Keywords: *FMCW radar, birds and drones spectrograms, wings flapping, drones rotors movement.*

1. INTRODUCTION

Today the importance of malicious drones detection grows every day. Various sensor types may be utilized for this task. A comprehensive survey of applied detection techniques is given in [1]. Among the detector types radars are unavoidable choice and an integral part of nearly all practical solutions.

Frequency Modulated Constant Wave (FMCW) radars are powerful device to detect and classify different objects. Such identification is based on the whole object movement or, at least, on some parts of object micro motion. These micro motions produce specific radar echo and, as a consequence, specific radar spectrograms depending on the characteristics of the observed object. For example, the obtained spectrograms as the result of drones' rotors rotation may be used for drones detection.

The spectrograms produced by drones' rotors rotation are often very similar to the spectrograms produced by birds' wings motion. Both directions in the sense of false detection are possible: 1. wings motion is detected as rotors rotation – false alarm, or 2. rotors rotation appears as wings motion – alarm miss. When drone presence is detected, its operation has to be jammed. Such scenario of jamming is called reactive jamming. (The other possible scenario is that jamming is performed continuously, regardless of drone detection process – this is active jamming [2], [3]).

Distinguishing drones and birds according to their spectrograms is subject of significant number of analysis. In fact, FMCW radar effectiveness in birds detection and classification was noticed even 50 years ago [4]. Such investigation is further expanded in [5] where it is presented a classification algorithm aimed at automatic recognition of bird targets using Artificial Neural Networks (ANN) (machine learning) principles. ANNs (i.e. its class Convolutional Neural Networks) have been analyzed in a mission of drones and birds distinguishing. Such solutions have proved high reliability in birds' and drones' targets differentiation with error probability in some scenarios significantly lower than 10% [6]. In contribution [7] micro-Doppler signatures are filtered to compensate Doppler shift caused by target (drone or bird) motion and to get only the spectrogram caused by micro motions as this is very powerful base for targets classification. The authors in [8] prove this statement, i.e. why it is worth to filter Doppler shift due to the whole target motion: the probability of successful detection drops down for moving objects caused both by their velocity and acceleration or, in other words, detection must take longer time for such objects. The most often applied frequency for FMCW radar realization is 24GHz (our analysis in this paper is limited to this frequency), but better quality spectrograms are usually obtained using higher radar frequencies (for example 94GHz in [9]). The lower frequencies are also applicable (9.6GHz in [8]). FMCW radars are not the only one to exploit Doppler-effect to obtain drones or birds spectrograms. They may be also obtained by pulsed-Doppler radars [10] although the appearance of spectrograms is different than in the case of FMCW radars application.

Analytical models of birds and drone flight are presented in the sections II and III. The spectrograms according to these models are drawn in the sections IV and V. The main suggestions how to distinguish birds and drones from the presented spectrograms are emphasized in the section VI. Finally, conclusions are in the section VII.

2. BIRD FLIGHT MODELLING

Wings motion is the cause of birds' micro-Doppler signatures. Depending on the view direction towards the FMCW radar, the wing motion may be modelled as flapping (Figure 1a), twisting (Figure 1b) or sweeping (Figure 1c). When a view is from the front or back side, besides only flapping, the wing may have one movement more, meaning that folding wing is obtained (Figure 1d) [11]. Generally, the view at the flying bird is not strictly according to the one of the positions from figures 1a, 1b or 1c. The method for spectrogram determination in such general case is presented in [12].

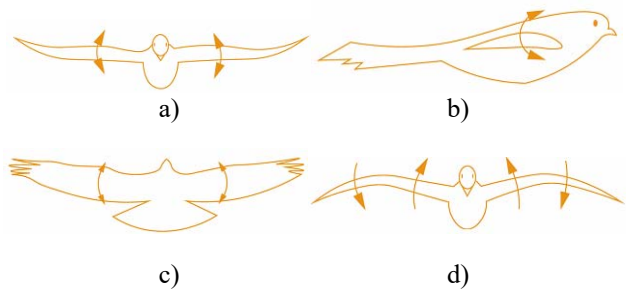

Figure 1. Modelling wings motion: a) flapping; b) twisting; c) sweeping; d) folding

Our contribution in this paper is to develop in a closed analytical form the expression for bird micro-Doppler signature. In the analysis we are limited to the case from the Figure 1a. The only bird motion is its wings flapping, the bird is nearly not flying.

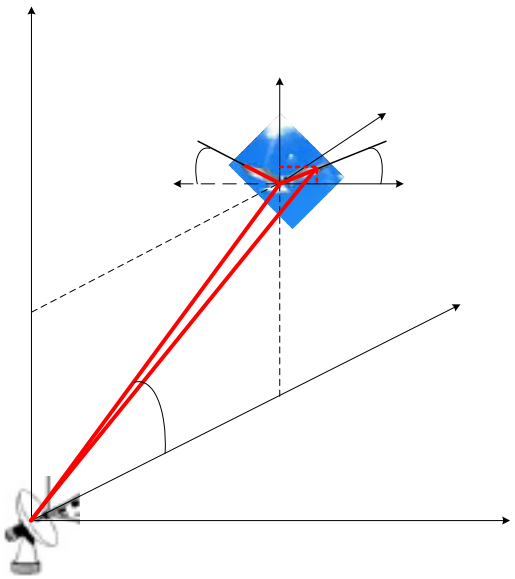

Figure 2. Parameters to determine bird micro-Doppler signature

We start from the sketch in the Figure 2. FMCW radar is located at the origin point of coordinate system xyz. The centre of the bird body is at the point where it is x_1=0 and the two remaining coordinated may be expressed as:

$$y_1 = R_0 \cdot \cos\beta \tag{1}$$

$$z_1 = R_0 \cdot \sin\beta \tag{2}$$

where R_0 is the distance between radar and the bird body central point A and β is the bird central point elevation towards the horizontal plane.

According to our model, flapping of wings is realized in the plane parallel to xz plane at the distance y_1. We shall suppose that the bird is located in the new coordinate system $x_a y_a z_a$ whose origin point has coordinates x_1=0 while y_1 and z_1 are expressed by (1) and (2). The wings angle φ during flapping may be modelled as

$$\varphi(t) = \varphi_{\max} \cdot \sin\left(2\pi \cdot f_{fl} \cdot t + \varphi_0\right) \tag{3}$$

where φ_{max} is the maximum flapping angle, f_{fl} is the flapping rate and φ_0 is the initial flapping angle. Without loss in generality we shall suppose that φ_0=0.

Let us now consider some point B on the bird wing at the distance l_p from the bird central point A. The coordinates of this point are expressed as:

$$x_2 = l_p \cdot \cos\varphi \tag{4}$$

$$z_2 = l_p \cdot \sin\varphi \tag{5}$$

The distance of point B from the FMCW radar may be now calculated as

$$\begin{aligned} OB = R_p &= \sqrt{x_2^2 + y_1^2 + (z_1 + z_2)^2} = \\ &\sqrt{l_p^2 \cdot \cos^2\varphi + R_0^2 \cdot \cos^2\beta + (R_0 \cdot \sin\beta + l_p \cdot \sin\varphi)^2} \\ &= \sqrt{l_p^2 + R_0^2 + 2 \cdot R_0 \cdot l_p \cdot \sin\beta \cdot \sin\varphi} \approx \\ &\approx R_0 + l_p \cdot \sin\beta \cdot \sin\varphi \end{aligned} \tag{6}$$

because it is

$$\left(\frac{l_p}{R_0}\right)^2 \approx 0 \tag{7}$$

and it is valid, generally

$$\sqrt{1 + 2 \cdot q} \approx 1 + q \tag{8}$$

for low values of q.

Now the radar received signal as a consequence of reflection from the point B is

$$\begin{aligned} s_R(t) = &\exp\left\{-j \cdot \left[2\pi \cdot f \cdot t + \frac{2\pi \cdot f}{c} \cdot 2 \cdot R_p(t)\right]\right\} = \\ &\exp\left\{-j \cdot \left[2\pi \cdot f \cdot t + \frac{4\pi}{\lambda} \cdot (R_0 + l_p \cdot \sin\beta \cdot \sin\varphi)\right]\right\} \end{aligned} \tag{9}$$

where f is the radar frequency, λ is its wavelength and the reflected signal passes the distance R_p two times. It is supposed that total transmitted signal is reflected towards radar.

The total reflected signal from one bird wing is obtained after integrating the reflected signal over the whole wing length L:

$$s_L(t) = \exp\left(-j\cdot\frac{4\pi}{\lambda}\cdot R_0\right)\cdot \cdot\int_0^L \exp\left\{-j\cdot\left[\frac{4\pi}{\lambda}\cdot\left(l_p\cdot\sin\beta\cdot\sin\varphi\right)\right]\right\}\cdot dl_p \quad (10)$$

Replacing (3) to (10) it is obtained

$$s_L(t) = \exp\left(-j\cdot\frac{4\pi}{\lambda}\cdot R_0\right)\cdot \cdot\int_0^L \exp\left\{-j\cdot\left[\frac{4\pi}{\lambda}\cdot \left(l_p\cdot\sin\beta\cdot \cdot\sin\left(\varphi_{\max}\cdot\sin\left(2\pi\cdot f_{fl}\cdot t+\varphi_0\right)\right)\right)\right]\right\}\cdot dl_p \quad (11)$$

If we now introduce the replacement

$$K = -\frac{4\pi}{\lambda}\cdot\sin\beta\cdot\sin\left(\varphi_{\max}\cdot\sin\left(2\pi\cdot f_{fl}\cdot t\right)\right) \quad (12)$$

it is obtained

$$s_L(t) = \exp\left(-j\cdot\frac{4\pi}{\lambda}\cdot R_0\right)\cdot\int_0^L \exp\left\{j\cdot K\cdot l_p\right\}\cdot dl_p = = L\cdot\exp\left(-j\cdot\frac{4\pi}{\lambda}\cdot R_0\right)\cdot e^{\frac{j\cdot K\cdot L}{2}}\cdot\sin c\left(\frac{K\cdot L}{2}\right) \quad (13)$$

where it is $\sin c(q_1)=\sin(q_1)/q_1$.

The movement of two bird's wings is symmetric towards the *yz* plane i.e. towards the radar meaning that both wings produce the same effect when considering spectrogram. Thus the total reflected signal from both wings is

$$s_{Ltot}(t) = 2\cdot s_L(t) \quad (14)$$

or the magnitude of this signal is

$$\left|s_{Ltot}(t)\right| = \left|2\cdot L\cdot\exp\left(-j\cdot\frac{4\pi}{\lambda}\cdot R_0\right)\cdot e^{\frac{j\cdot K\cdot L}{2}}\cdot\sin c\left(\frac{K\cdot L}{2}\right)\right| \quad (15)$$

The standard procedure to calculate spectrogram is based on Short Time Fourier Transform (*STFT*) calculation of the considered signal according to the equation [13]:

$$STFT\left(S_n(m,\omega)\right) = \sum_{n=-\infty}^{\infty} S_n\cdot w_{n-m\cdot R}\cdot\exp\left(-j\cdot\omega\cdot t_n\right) \quad (16)$$

where R is the number of samples between two successive segments of Fourier transform calculation, m is the ordinary number of a segment and w_n is the Hanning window defined by [14]:

$$w_n = \frac{1}{2}\cdot\left(1-\cos\frac{2\cdot\pi\cdot n}{N}\right)\quad (n=0,1,2...N) \quad (17)$$

If we now analyze the expression (15) and, related to it, the expression (12), we conclude that four elements contribute to the birds micro-Doppler signature appearance: the elevation angle β, the maximum flapping angle φ_{max}, the flapping rate f_{fl} and the wings length L.

3. DRONE FLIGHT MODELLING

Method for drone micro-Doppler signature calculation has been already developed in [12], [15]. The developed model considers separately single rotor and multirotor drones. On the base of these contributions we have already performed the analysis of various drone micro-Doppler signatures in [16]. This analysis is limited to hovering drones, i.e. drones which are not flying. In order to consider a higher number of spectrograms and the influence of wider range of characteristic parameters change, we have developed our original calculation program [17]. Here we only repeat the formula for the magnitude of the single rotor drone echo signal:

$$\left|S_\Sigma(t)\right| = \left|L\cdot\exp\left(-j\frac{4\cdot\pi}{\lambda}\cdot\left(R_0+z_2\cdot\sin\beta\right)\right)\cdot \cdot\sum_{k=0}^{N-1}\sin c\left(\Phi_k(t)\right)\cdot\exp\left(-j\cdot\Phi_k(t)\right)\right| \quad (18)$$

as well as for multi rotor drone echo signal:

$$\left|S_\Sigma(t)\right| = \left|\sum_{i=1}^{N_r}\sum_{k=0}^{N-1} s_{lk}(t)\right| = \left|\sum_{i=1}^{N_r} L\cdot\exp\left(-j\frac{4\cdot\pi}{\lambda}\cdot\left(R_{0i}+z_{2i}\cdot\sin\beta_i\right)\right)\cdot \cdot\sum_{k=0}^{N-1}\sin c\left(\Phi_{ik}(t)\right)\cdot\exp\left(-j\cdot\Phi_{ik}(t)\right)\right| \quad (19)$$

where it is

$$\Phi_{ik}(t) = \frac{4\cdot\pi}{\lambda}\cdot\frac{L}{2}\cdot\cos\beta_i\cdot\cos\left(\Omega_i\cdot t+\varphi_{0i}+\frac{2\cdot\pi\cdot k}{N}\right)\quad (k=0,1,2,...N\text{-}1) \quad (20)$$

The meaning of the new variables in (18)-(20) comparing to the previous formulas is:

- N - the number of blades in each rotor;
- Ω - rotor angular rotation speed;
- N_r - the number of drone rotors.

The maximum Doppler shift may be calculated as [12]

$$f_{D\max} = \frac{4\cdot\pi\cdot\Omega\cdot L}{\lambda}\cdot\cos\beta \quad (21)$$

4. BIRDS' SPECTROGRAMS CAUSED BY FLAPPING WINGS

Several birds spectrograms, obtained when four already cited parameters in the Section 2 are varied are presented in the figures 3-X. The graphs in these figures are now obtained starting from the echo magnitude expressed by (15) which is then modified using (16) and (17) to give the desired time-frequency shape. All spectrograms in the paper are presented for FMCW radar operating frequency f=24GHz and digital sampling rate f_{step}=20kHz. Generally, all spectrograms have the similar describable

appearance: the parts with higher echo (wider brown, red, orange and yellow areas) are periodically followed by the parts with lower echo where brown, red, orange and yellow areas are narrower. The rate of these areas in spectrogram corresponds to the bird wings flapping rate. The frequency bandwidth of the wider areas depends on the concrete values of four parameters.

The influence of β is obvious according to the figures 3 and 4. The values of four variable parameters are presented by different colour ink for each parameter in the figures' legend. The bandwidth of wider frequency areas is increased when β, i.e. arcsin(β) is increased. An explanation of such behaviour follows from the fact that bird wings are flapping in *yz* plane. Thus the variation of their distance from radar is maximum when it is β=90°. When it is β=0°, this variation practically does not exist.

The influence of wings length may be analyzed comparing figures 4 and 5. It is obvious the logical conclusion that longer wings lead to wider frequency area with brown, red, orange and yellow colour.

Influence of maximum flapping angle follows from the comparison of figures 4 and 6. The greater flapping angle also means that frequency area with brown, red, orange and yellow colour will be wider.

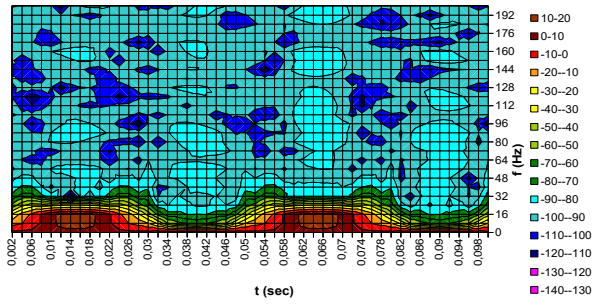

Figure 3. Spectrogram of bird with flapping wings, the wing length ***L*=0.24m**, wing flapping rate f_{fl}**=20flaps/s**, maximum flapping angle φ_{max}**=40°**, bird height z_1=30m, bird distance from radar R_0=100m, bird elevation angle towards radar β**=arcsin(0.3)**.

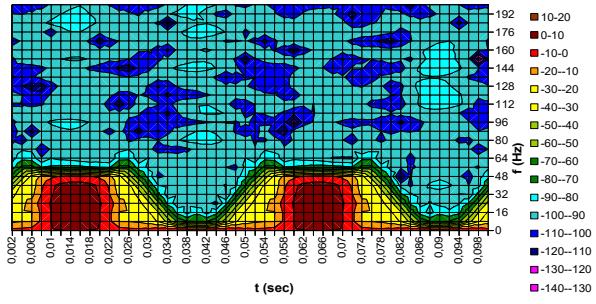

Figure 4. Spectrogram of bird with flapping wings, the wing length ***L*=0.24m**, wing flapping rate f_{fl}**=20flaps/s**, maximum flapping angle φ_{max}**=40°**, bird height z_1=70m, bird distance from radar R_0=100m, bird elevation angle towards radar β=arcsin**(0.7)**.

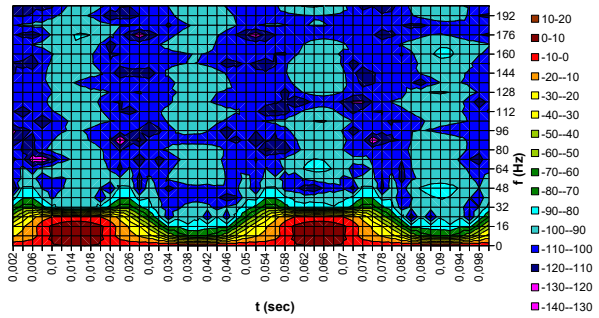

Figure 5. Spectrogram of bird with flapping wings, the wing length ***L*=0.12m**, wing flapping rate f_{fl}**=20flaps/s**, maximum flapping angle φ_{max}**=40°**, bird height z_1=70m, bird distance from radar R_0=100m, bird elevation angle towards radar β=arcsin**(0.7)**.

Variation of flapping rate has twofold effect onto spectrogram as may be concluded after the comparison of figures 6 and 7. The number of spectrogram figures repetitions equals the flapping rate, but also the bandwidth of brown, red, orange and yellow colour area increases when the flapping rate increases.

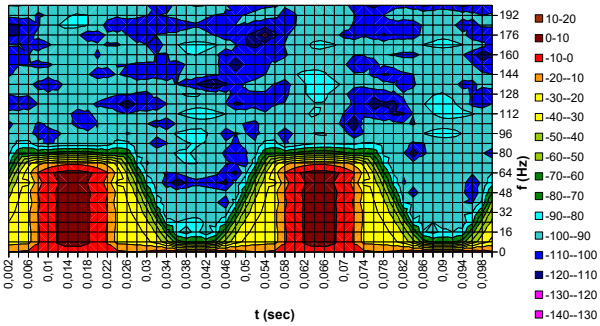

Figure 6. Spectrogram of bird with flapping wings, the wing length ***L*=0.24m**, wing flapping rate f_{fl}**=20flaps/s**, maximum flapping angle φ_{max}**=60°**, bird height z_1=70m, bird distance from radar R_0=100m, bird elevation angle towards radar β**=arcsin(0.7)**.

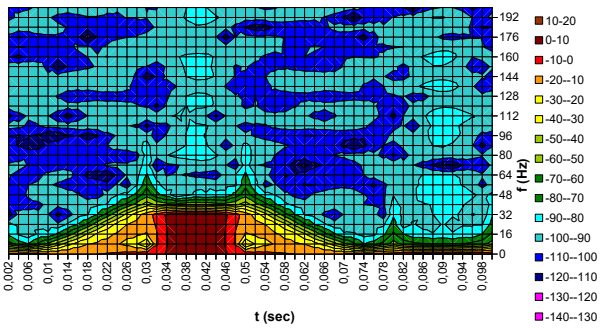

Figure 7. Spectrogram of bird with flapping wings, the wing length ***L*=0.24m**, wing flapping rate f_{fl}**=10flaps/s**, maximum flapping angle φ_{max}**=60°**, bird height z_1=70m, bird distance from radar R_0=100m, bird elevation angle towards radar β**=arcsin(0.7)**.

5. DRONES' SPECTROGRAMS CAUSED BY ROTORS MOVEMENT

Drones spectrograms are obtained using equation (18) or (19) depending on the number of drone's rotors. As for birds, the applied equation is then translated to time-frequency field by (16) and (17).

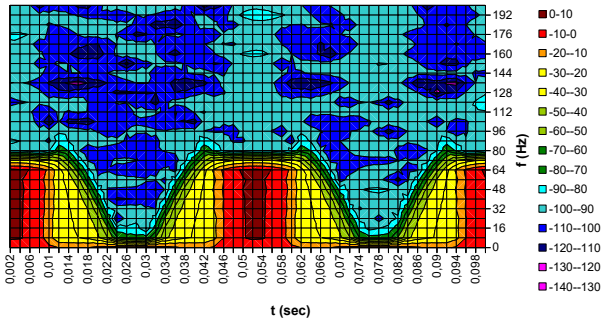

Figure 8. Drone spectrogram for **one rotor** with **one blade**, the blade length ***L*=0.24m**, blade rotation speed $\boldsymbol{\Omega_{rot}}$**=20rotations/s**, drone height h=70m, drone distance from radar R_0=100m, drone elevation angle towards radar $\boldsymbol{\beta}$**=arcsin(0.7)**.

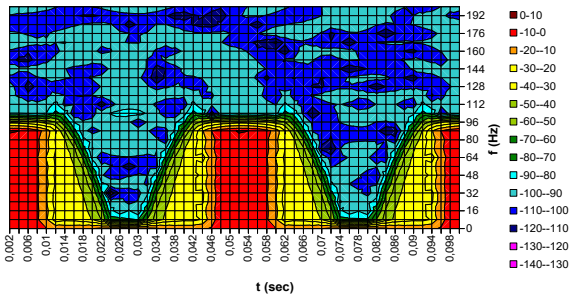

Figure 9. Drone spectrogram for **one rotor** with **one blade**, the blade length ***L*=0.24m**, blade rotation speed $\boldsymbol{\Omega_{rot}}$**=20rotations/s**, drone height h=30m, drone distance from radar R_0=100m, drone elevation angle towards radar $\boldsymbol{\beta}$**=arcsin(0.3)**.

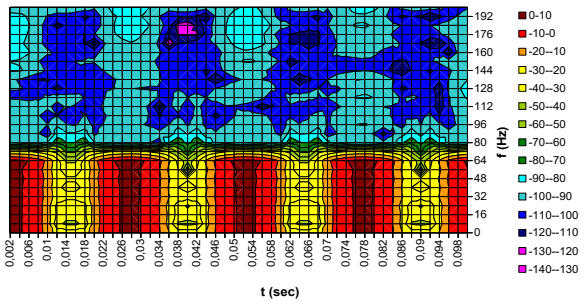

Figure 10. Drone spectrogram for **one rotor** with **two blades**, the blade length ***L*=0.24m**, blade rotation speed $\boldsymbol{\Omega_{rot}}$**=20rotations/s**, drone height h=70m, drone distance from radar R_0=100m, drone elevation angle towards radar $\boldsymbol{\beta}$**=arcsin(0.7)**.

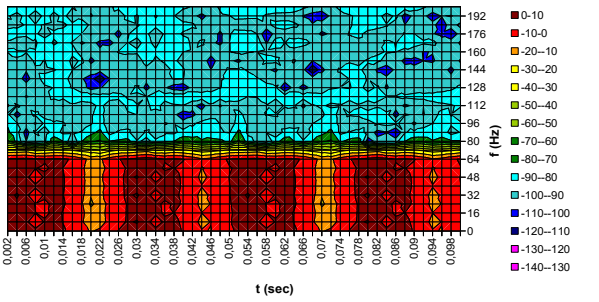

Figure 11. Drone spectrogram for **four rotors** with **one blade**, the blade length ***L*=0.24m**, blade rotation speed $\boldsymbol{\Omega_{rot}}$**=20rotations/s**, drone height h=70m, drone distance from radar R_0=100m, drone elevation angle towards radar $\boldsymbol{\beta}$**=arcsin(0.7)**.

The influence of elevation angle β is opposite than in case of birds. It is illustrated by the spectrograms in the figures 8 and 9. The bandwidth of wider frequency areas is decreased when β, i.e. arccos(β) is increased. An explanation of such behaviour follows from the fact that drone rotors are rotating in xy plane. Thus the variation of their distance from radar is maximum when it is β=0°. When it is β=90°, this variation practically does not exist.

Characteristics of drone spectrograms are modified in the same way when rotor blades length and their rotation rate are varied as when bird wings length and flapping rate are changed. That's why these characteristics are not presented in this paper.

When rotor drone has two blades, the frequency of repeated areas with wider brown, red, orange and yellow parts is doubled, as presented in the Figure 10. If the number of rotors is increased instead of the number of rotor blades (quadcopters are very often applied), spectrogram changes its appearance. It has one more uniform area, without separated brown, red, orange and yellow parts. This is presented by the Figure 11.

6. DRONES AND BIRDS DETECTION FROM THEIR SPECTROGRAMS

The following steps about drone or birds target presence may be defined on the base of investigation presented in this paper:

1. spectrograms of multirotor drones (quad or more) are highly different and the possibility of false detection is very small. Hovering quadcopter's spectrogram more looks like one surface of uniform bandwidth (brown, red and orange surface in the Figure 11). All spectrograms of birds with flapping wings have sinusoidal repetition of such surfaces (for example, the spectrogram in the Figure 4 is for the same β, same L and the value of f_{fl} is the same as the value of Ω_{rot} for the drone in the Figure 11);
2. if difference may not be made according the step 1, i.e. if the drone target is of helicopter type, it is necessary to go to the further steps. The second step in the decision algorithm is to determine the rate of spectrogram repetitions. The drones' rotors rotation

rate is usually higher than the birds' wings flapping rate [15]. In the case that helicopter's rotor has more than one blade, the rate of spectrogram repetitions is even obtained by the multiplication of the rotation rate and the number of blades (Figure 10 for two blades). Such behaviour means that the probability of false detection when it is necessary to distinguish birds and helicopter drones with the rotor having more than one blade is further decreased;

3. the third criterion of decision could be implemented for helicopter drones having only one blade in their rotor (which is very rare case). It is necessary to consider in the same time the target elevation angle β and the bandwidth of the spectrogram part in brown, red, orange and yellow colour. Our investigation has proved that this bandwidth increases when birds are considered, but decreases when drones are considered, as a function of β increasing (figures 3 and 9). We have explained that the difference of plane where micro motions is performed is the cause of this characteristic behaviour. As a consequence, it is possible to make a reliable decision about the detected target when β is gradually increased (as a consequence of target approaching at nearly same height) or decreased;
4. it remains now to analyze the situation when the target is moving directly towards radar. In this case detection reliability may be improved by considering maximum flapping angle φ_{max}. According to [12], the typical value of this angle is 40º and with such angle the obtained bandwidth of brown, red, orange and yellow surface is lower than for drone spectrogram (figures 4 and 8).

The elevation angle β may be determined by the implementation of some algorithm on FMCW radar [17].

The possibilities for reliable distinguishing of birds from drones are here analyzed in a qualitative sense.

7. CONCLUSION

The main objective of this paper has been to define the algorithm to differ drones from birds when a target is detected. The decision is made based on the difference in the appearance of spectrograms collected by FMCW radar. The analysis is limited to hovering drones and birds with flapping wings. The obtained results, i.e. obtained spectrograms for drones may be easily compared to the corresponding recorded spectrograms presented in literature [12], [15]. The spectrogram shape dependence is based on the same drone construction and flight characteristics (number of blades in rotors, blades length, rotors rotation rate, etc.) and the spectrograms appearance is very similar in our paper as in this emphasized literature. Instead of practical measuring and recording, we have used our original calculation method to obtain the spectrograms based on varying the parameters of drones' and birds' flight. We have developed the expressions for modelling the bird moving and have used the already existent expressions for the drone. The results of our investigation show that there is possibility to easily distinguish birds from multirotor drones. In the case of drones with only one rotor (helicopter), differences in spectrograms are very clear when the drone has more than one blade and if its elevation angle is not in the area about 45º. There is only very low possibility of false detection when helicopter rotor has one blade and a drone is positioned near β=45º. The quantitative values for the decision algorithm and the collection of results by calculation and real-life recording will be the subject of future development.

References

[1] MATIĆ,V., KOSJER,V., LEBL,A., PAVIĆ,B., RADIVOJEVIĆ,J., *Methods for Drone Detection and Jamming*, 10th International Conference on Information Society and Technology (ICIST), Kopaonik, in: ZDRAVKOVIĆ, M., KONJOVIĆ, Z., TRAJANOVIĆ, M., Proceedings 1 (2020) 16-21.

[2] RADIVOJEVIĆ,J., PAVIĆ,B., LEBL,A., PETROVIĆ,M., *Sweep Jamming with Discrete Subbands – an Advanced Strategy for Malicious Drones Missions Prevention*, Scientific Technical Review, 71(2), (2022) 46-52, ISSN: 1820-0206, UDK: 355.43:623.624,449.8, COSATI: 03-10, 14-04-01, DOI: 10.5973/str2102046R.

[3] RADIVOJEVIĆ,J., LEBL,A., MILEUSNIĆ,M., VUJIĆ,A., ŠEVIĆ,T., JOKSIMOVIĆ,V., *Multichannel Radio-jammer Development Considerations for prevention of Illicit Drone Missions*, 9th International Scientific Conference on Defensive Technologies OTEH 2020., Belgrade (2020) 270-275, ISBN 978-86-81123-83-6.

[4] MARTISON,L.W., *A Preliminary Investigation of Bird Classification by Doppler Radar*, RCA Government and Commercial Systems, Missile and Surface Radar Division, Moorestown, NJ, NASA Wallops Station, Wallops Island, (1973).

[5] ZAUGG,S., SAPORTA,G., VAN LOON,E., SCHMALJOHANN,H., LIEHTI,F., *Automatic identification of bird targets with radar via patterns produced by wing flapping*, Journal of the Royal Society, 5, (2008) 1041-53, DOI: 10.1098/rsif.2007.1349.

[6] CHEN, X., ZHANG, H., SONG, J., GUAN, J., LI, J., HE, Z., *Micro-Motion Classification of Flying Bird and Rotor Drones via Data Augmentation and Modified Multi-Scale CNN*, Remote Sensing, 14, 1107, (2022) 1-25, https://doi.org/10.3390/rs14051107.

[7] MOLCHANOV,P., HARMANY,R.I.A., DE WIT,J.J.M., EGIAZARIAN,K., ASTOLA,J., *Classification of small UAVs and birds by micro-Doppler signatures*, International Journal of Microwave and Wireless Technologies, 6(3-4) (2014) 435-444.

[8] YOON,S.-W., KIM,S.-B., JUNG,J.-H.,CHA,S.-B., BACK,Y.-S., KOO,B.-T., CHOI,I.-O., PARK,S.-H., *Efficient Classification of Birds and Drones Considering Real Observation Scenarios Using FMCW Radar*, Journal of Electromagnetic Engineering and Science, 21(4) (2021) 270-281., ISSN: 2671-7255., https://doi.org/10.26866/jees.2021.

[9] RAHMAN,S., ROBERTSON,D.A., *Radar micro-Doppler signatures of drones and birds at K-band*

and W-band, Scientific Reports, (2018) 1-11, DOI: 10.1038/s41598-018-35880-9.

[10] RITCHIE,M., HORNE,C., PETERS, N., *Radar UAV and Bird Signature comparisons with Micro-Doppler*, Chapter 1, pp. 1-33.

[11] SONG,B., LANG,X., XUE,D., YANG,W., *A review of the research status and progress on the aerodynamic mechanism of bird wings*, Scientia Sinica Technologica, (2021) 1-18, DOI: 10.1360/SST-2020-0515.

[12] CHEN,V.C., *The Micro-Doppler Effect in Radar*, Artech House, Second Edition, 2019., ISBN: 978-1-63081-546-2.

[13] AHMADIZADEH,M., *An Introduction to Short-Time Fourier Transform (STFT)*, Sharif University of Technology, Department of Civil Engineering, (2014).

[14] GABERSON,H.A., *A Comprehensive Windows Tutorial*, Sound and Vibration, Instrumentation Reference Issue, (2006) 14-23.

[15] ZHAO,C., LUO,G., WANG,Y., CHEN,C., WU,Z., *UAV Recognition Based on Micro-Doppler Dynamic Attribute-Guided Augmentation Algorithm*, Remote Sensing, Article 1205, 13(6), (2021) 1-17., DOI: https://doi.org/10.3390/rs13061205.

[16] LEBL,A., MILEUSNIĆ,M., MITIĆ,D., RADIVOJEVIĆ,J., MATIĆ,V., *Verification of Calculation Method for Drone Micro-Doppler Signature Estimation*, accepted for publication in Facta Universitatis, Series: Electronics and Energetics, ISSN: 0353-3670.

[17] RADIVOJEVIĆ,J., PETROVIĆ,P., LEBL,A., MILEUSNIĆ,M., *Initial Development of a Program for Drone Micro-Doppler Signature Modelling*, on the review for the IXth IcETRAN Conference, Novi Pazar (2022).